ISTANBUL TECHNICAL UNIVERSITY ★ FACULTY OF AERONAUTICS AND ASTRONAUTICS

STRUCTURAL HEALTH MONITORING APPLICATIONS FOR GLASS FIBER REINFORCED COMPOSITES WITH CNT/CNC SENSORS

GRADUATION PROJECT

Hilal Erkoç

Department of Aeronautical Engineering

Anabilim Dalı : Herhangi Mühendislik, Bilim
Thesis Advisor: Doç. Dr. Hülya Cebeci
Programı : Herhangi Program

July, 2020

ISTANBUL TECHNICAL UNIVERSITY ★ FACULTY OF AERONAUTICS AND ASTRONAUTICS

STRUCTURAL HEALTH MONITORING APPLICATIONS FOR GLASS FIBER REINFORCED COMPOSITES WITH CNT/CNC SENSORS

GRADUATION PROJECT

Hilal Erkoç
110160713

Department of Aeronautıcal Engineering

Thesis Advisor: Doç.Dr. Hülya Cebeci
Anabilim Dalı : Herhangi Mühendislik, Bilim
Programı : Herhangi Program

JULY 2020

Hilal Erkoç, student of ITU Faculty of Aeronautics and Astronautics student ID 110160713, successfully defended the **graduation** entitled "**STRUCTURAL HEALTH MONITORING APPLICATIONS FOR GLASS FIBER REINFORCED COMPOSITES WITH CNT/CNC SENSORS"**, which she prepared after fulfilling the requirements specified in the associated legislations, before the jury whose signatures are below.

Thesis Advisor:	**Doç. Dr. Hülya Cebeci** Istanbul Technical University	.....
Jury Members:	**Prof. Dr. İbrahim Özkol** Istanbul Technical University	.....
	Doç. Dr. Aytaç Arıkoğlu Istanbul Technical University	.....

Date of Submission: 13 July 2020
Date of Defense: 21July 2020

To my family,

FOREWORD

I would like to appreciation to my supervisor, Assist. Prof. Dr. Hülya Cebeci, for contributing valuable and inspiring advices while all my undergraduate life. Furthermore, I would like to thank Fırat Turgut for helps and support me. I present my gratitude to my family who believed and supported me throughout my life.

July 2020 HİLAL ERKOÇ

Table of Content

ABBREVIATION

SHM	**:** Structural Health Monitoring
CNT	**:** Carbon Nanotube
CNC	**:** Cellulose Nanocrystalls
POD	**:** Probability of Detection
MWCNT	**:** Multiwall Carbon Nanotube
SWCNT	**:** Singlewall Carbon Nanotube
GFRP	**:** Glass Fiber Reinforced Polymer
CFRP	**:** Carbon Fiber Reinforced Polymer

LIST OF TABLES

LIST OF FIGURES

THESIS TITLE IN ENGLISH HERE

SUMMARY

Fiber reinforced polymer matrix composite materials are used in many fields such as aviation, automotive, and marine. Depending on the developing technology, the demand for light, durable and reliable materials is increasing day by day. Serious studies are carried out on advanced and nano-reinforced composite materials to meet these demands and to carry out innovative applications. Despite their superior properties such as composite materials, high mechanical properties and lightness, resistance to chemical and environmental conditions, they show great problems in damage formation and damage progress due to their layered structure. Crack progression is very difficult to follow in composite materials, and damage to the intermediate layers cannot be detected by simple methods such as visual inspection, and special inspection methods must be used for these. One of the most common problems in the aviation industry is that the parts are damaged due to fatigue. The parts used get tired when they are subjected to repeated loads, and when a load is applied over a certain limit, they are subject to sudden and permanent damage. This damage can cause serious accidents when it occurs between scheduled maintenance periods. In addition, when the operational costs are evaluated, maintenance and repair expenses constitute a large part of it. Inspections performed for control purposes without any damage repairs mean unnecessary costs. Considering all these situations, the use of concurrent structural health monitoring methods to carry out both reliable and economical operations is of great importance for commercial applications.

Although commercially used strain gauge and fiber optic sensor applications are economical, they cannot be used efficiently as they do not provide sufficient information in large-scale structures. Therefore, studies are carried out to develop simultaneous structural health monitoring methods. The most striking of these is the use of carbon nanotubes (CNT), which have many uses, with their versatile properties in structural health examination methods. In this study, a special paint was produced with CNT/CNC solution and the antenna pattern was printed on the composite plate by screen printing method. The effect of the resonance frequency of the antenna pattern on dimensional changes has been investigated. It has been observed that the resonance frequency decreases with elongations.

1. INTRODUCTION

1.1. Advanced Composites for Aerospace Applications

Composite materials have a wide range of uses, and their use is rapidly increasing. Composites whose properties can change according to the purpose and place of use can be tailored to meet special needs such as high strength and stiffness combined with light weight. The resulting high-performance materials are increasingly being used in aircraft, space and defense applications. There are many types of composite materials. Of these, the type that has the most common usage in the aeronautical industry is glass fiber reinforced polymers (GFRP). GFRP composites are widely used in the aeronautical and the automotive industry mainly due to their high specific mechanical properties. Even their high in plane properties composites have weaknesses on compression and interlaminar properties**.** Further, performance of composite materials may be decrease when damage occurs in structure. During the last decades, the aerospace industry focuses its research in producing multi-functional materials, driving design parameters being the weight reduction with increased mechanical properties as well as monitoring their structural health by means of sensing capability [1].

Damage in composite materials occurs in many more ways. The anisotropic nature of the composite laminates induced by the fragile fibers and the ductile resins as well as the low interlaminar strength, contributes to the facing challenges generally including delamination and micro cracks (Figure 1.1) during the service stage, especially when suffering from mechanical and thermal stress [2].

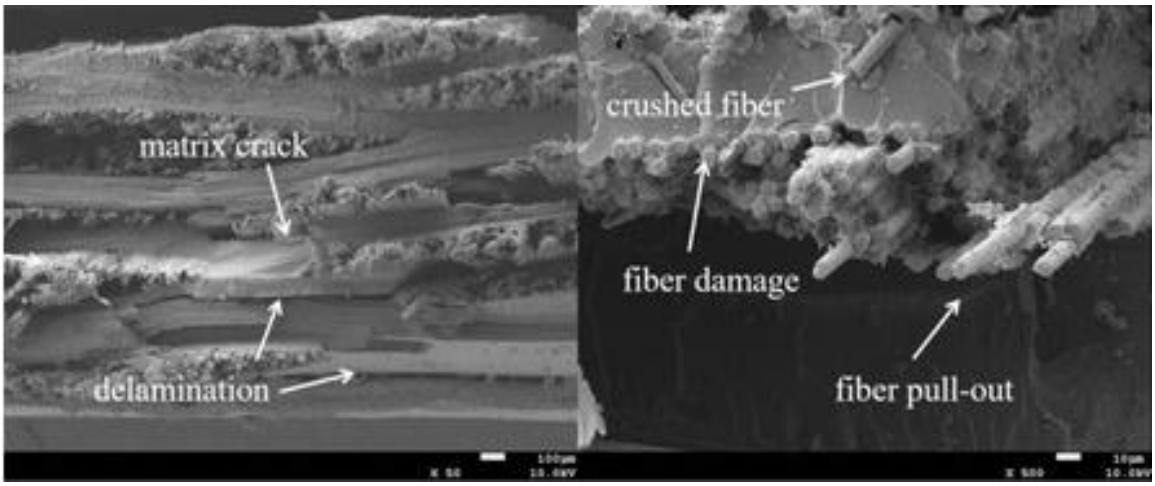

Figure 1 :Composite Damage Types

Since reliability is a prerequisite for the aviation industry, the maintenance procedures set by the aviation authorities must be followed to keep an aircraft in airworthy. Aircraft maintenance procedures require checking the structural condition of the aircraft. Therefore, it should be checked by various methods that there is no damage to the structural parts of the aircraft and that parts are in suitable condition. The composites are prone to hidden damage from low-velocity impact (e.g., the drop of a hand tool on a wing, or large hail impact on a radome); such damage can be barely visible and may go undetected, but its effect on the degradation of the composite structure strength can be dramatic [3]. Detecting this kind of damages which occurs under the surface of composite materials is hard, this condition makes aircraft maintenance difficult and prolongs the maintenance process.

Structural health monitoring is procedure of determining the stress and strain states of a structure in order to detect and locate sites of damage. Other damage measuring methods based on large area measurements (ultrasonic Cscans, scanning Doppler laser velocimetry, thermography, etc.) have been used in SHM development for definition and confirmation of damage and/or for understating the proposed SHM approach; however, they do not seem appropriate for permanent installation onto the monitored structure [4]. Structural health monitoring (SHM) relies on sensors that can be permanently placed on the structure and
monitored over time either in a passive or in an active way.
There are many SHM methods such as conventional resistance strain gages, fiber-optic sensors, fiber Bragg grating methods. However, these methods are difficult to

integrate into the structure and have low sustainability. Therefore, in this study structural health monitoring will be carried out by printing a special pattern with a CNT / CNC solution on the structure in order not to cause any deterioration in the structure

2. LITERATURE REVIEW

2.1. Structural Health Monitoring

Airplanes are exposed to various stresses during their operations. Further, many damages can occur due to bird hit, lightning strike, tool drop, ground handling etc. As a result of these effects, some failures such as delamination, cracks or fiber pull out may occur in the composite structure of the aircraft. These failures must be detected and repaired and when it's required parts substitute new one without causing major problems.

Structural Health Monitoring (SHM) is the system that monitoring of the structural situations simultaneously and provides instant maintenance triggers when system health drops below a predefined confidence level. The main purpose of the SHM system is to monitor damage and load conditions that have a direct influence on the aircraft's suitability for service. SHM system contains many functions such as detection of unanticipated damages, damage location identification, damage characterization through imagining, monitoring damage growth and enabling feedback action/alarm mechanism.SHM system makes embedded non-destructive testing sensors an integral part of structure and operates with minimal manual intervention [5].

SHM system include three steps:

1. Diagnosis
2. Prognosis
3. Predictive Maintenance and Life Extension

Diagnosis is the stage of monitoring the structural health status of the area under inspection. In the diagnostic phase, wired or wireless sensors which are spread over a wide area of the structure are used. Periodic measurements are taken from in-situ sensors to a central analysis station in the system via wired or wireless media.

In the prognosis phase the inspection data received in the diagnosis phase is analyzed and estimated whether there is any damage to the interior or exterior parts of the structure. Estimated damage properties are used in damage development models to find a requirement to predict the remaining life of the structure and trigger maintenance. Damage estimation models are effectively combined with the probability of detection (POD) models for structural integrity assessment and residual life estimation [5].

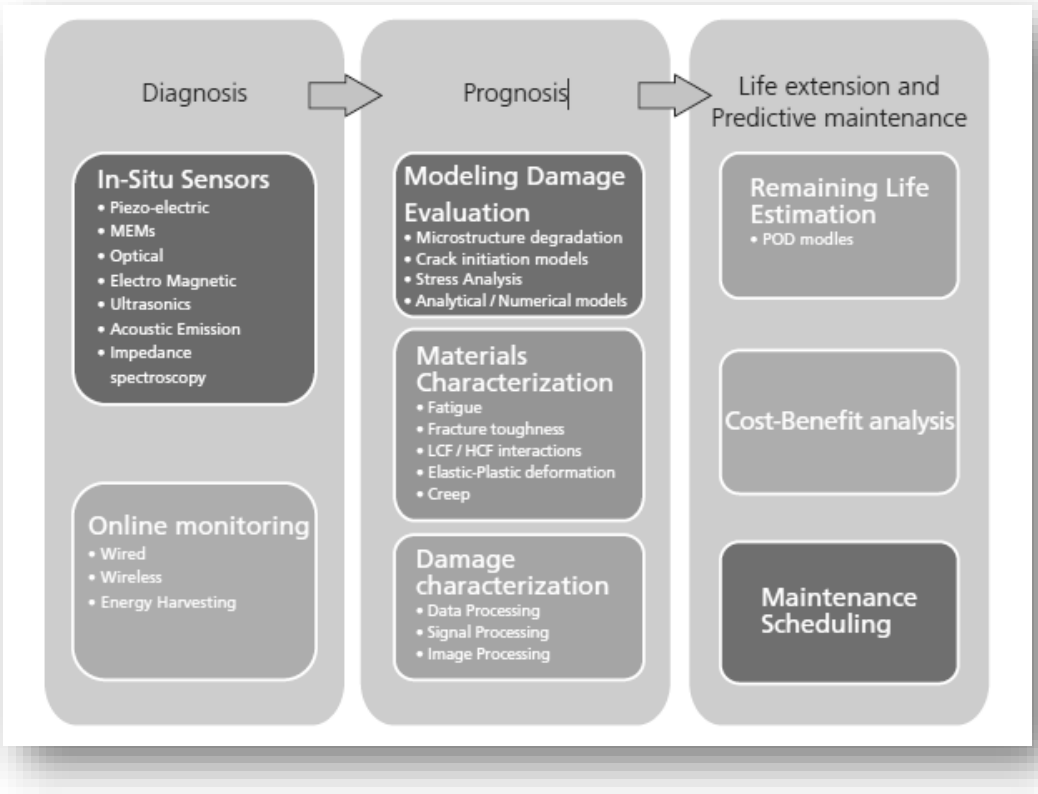

Figure 2 : Probability of Detection Models

2.2 Sensors for SHM of Aerospace Composites

Some of the types of sensors used for SHM applications are:

1. Conventional resistance strain gages
2. Fiber-optic sensors, e.g., fiber Bragg gratings (FBG) strain sensors
3. Piezoelectric wafer active sensors (PWAS)
4. Electrical property sensors: resistance, impedance, dielectric, etc.

These sensors can operate in static and dynamic regimes, depending on the physical principle used to monitor the structure.

2.2.1 Conventional Resistance Strain Gages

Conventional resistance strain gages have been using since the mid-1900s and have wide recognition in experimental stress analysis. Its physical principles are to transform a relative strain change into a relative resistance change that is read with a sensitive instrument (e.g. a Wheatstone bridge). The strain- induced resistance change may originate from either changes of geometric properties (e.g. foil strain gages) or piezo resistive effect provided by electronic materials. Strain gages working principle can be expressed by that relation:

$$\frac{\Delta R}{R} = S_g \Delta\varepsilon + S_T \Delta T + S_t \Delta t$$

S_g = Gage sensitivity to strain (a.k.a. gage factor)

S_T = Gage sensitivity to temperature

S_t = Gage sensitivity to time

Strain gages manufacturers aim to minimize time and temperature effect to resistance changes. Main purpose is observation of resistance changes which provided by strain.

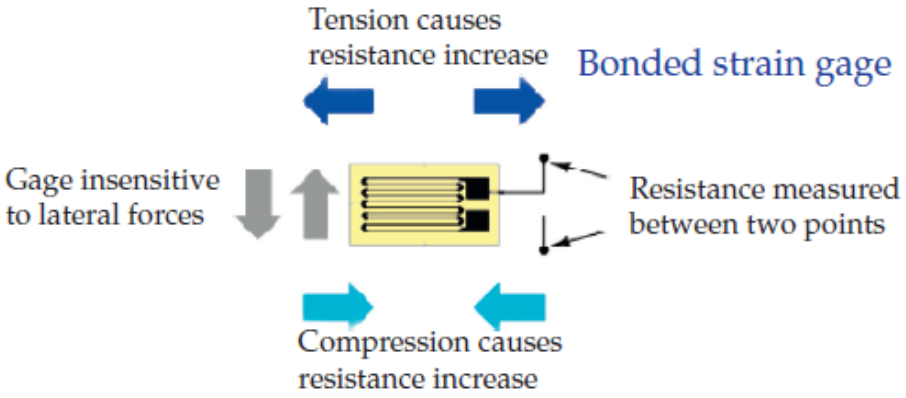

Figure 3 : Strain gage fundamentals: schematic of strain gage mode of operation

Attention should be paid to the adhesion between the composite and strain gages in the application of strain gages on the composite. If the adhesion problem occurs between the surfaces, correct results cannot be obtained. In composite structures, we can place strain gages inside the structure for example we can put strain gages between composite layers. But in this case, we have problems with the placement of the strain gage's cables. We may need to drill holes in the composite to lay the cables, which reduces the strength of the composite structure.

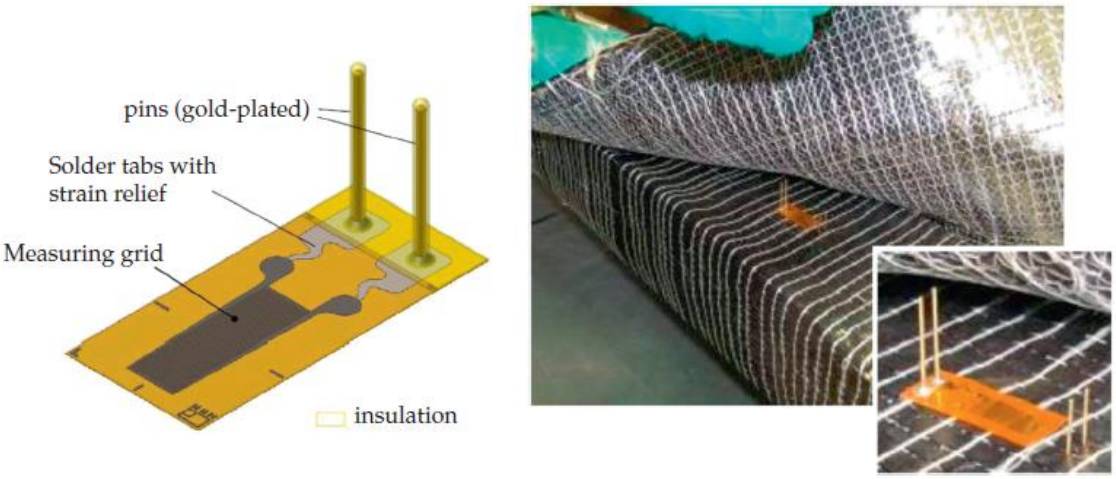

Figure 4: Strain Gages Applications

In addition, bandwidth of the electronic conditioning equipment limits he signal bandwidth, due to the strain gauge converts directly the strain change into a resistance change [4]. New SHM methods have been developed instead of strain gages due to wiring challenges, narrow available signal range and weakening of the connection with the surface when exposed to temperature changes.

2.2.2 Fiber Optic Sensors

The working principle of fiber optic detection is due to the reflection of light. Light spreads as an electromagnetic wave among the optical fiber. Optical fibers consist of a cen b tral core region surrounded by a circular coating. The light guiding properties of optical fibers are associated with the phenomenon of total internal reflection which is because of the difference between the cladding and core refractive indices

$n_{cladding} < n_{medium} < n_{core}$ [7] Total internal reflection evaluates at the interface between the high-index core and lower-index cladding.

Snell's law implemented to these different refractive indices yields the result that no transmission in the cladding is possible and therefore the light wave reflects back into core.

Therefore, the light traveling in an optical fiber is restricted to core. Consequently, light can travel large distances over an optical fiber with extremely little decrement.

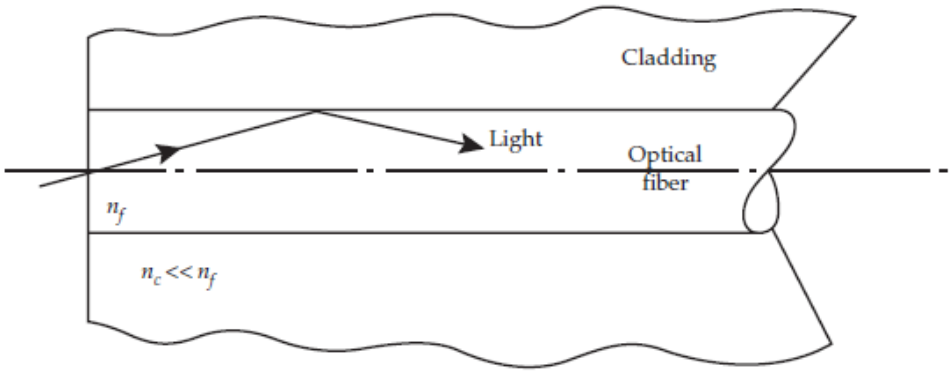

Figure 5:Principle of total internal reflection in an optical fiber.

There are four fiber-optic sensing mechanisms for SHM applications:

I. Intensity modulation
II. Phase modulation
III. Spectral modulation (Fabry-Perot interferometers (FPI) and fiber Bragg gratings (FBG))
IV. Polarization modulation

Fiber Optic Sensors provide some advantages for SHM such as;

1. Immune to electromagnetic interference (EMI)
2. Corrosion resistance
3. Possibility of multiplexing several sensors on the same optical fiber
4. The promise of direct embedment into the composite material along the reinforcing fibers

Fiber-optic sensors also have some penalties that have interrupted their extensive usage;

1. It requires remarkable optoelectronic equipment to transform the optical changes into actual readings of the physical quantity being monitored (strain, or other material property)
2. The limited bandwidth due to the optoelectronic equipment that has to perform complicated processing of the optical signal

Although integrating fiber optic sensors into the composite structure seems to be a very attractive way, the diameter of the typical telecom optical fiber is usually in the range of 120 and 250 μm, and integrating a fiber optical fiber of this diameter into the structure can adversely affect the structural properties and integrity of the composite. Small-diameter optical fibers (e.g., 52 μm) has developed for composite SHM embedment, however these specialty fibers are too expensive than the run-of-the-mill telecom fibers [8].

2.2.3 Piezoelectric Wafer Active Sensors (PWAS)

Piezoelectric wafer active sensors (PWAS) are inexpensive and convenient low-profile transducers. PWAS have been used broadly in guided-waves structural health monitoring (SHM) of aerospace composites. PWAS transducers are produced of thin piezo ceramic wafers electrically poled in the thickness direction. The integration of PWAS into the structure can be done easily like strain gages. However, it is a disadvantage that the structure decreases structures mechanical properties if it is placed in interlayers.

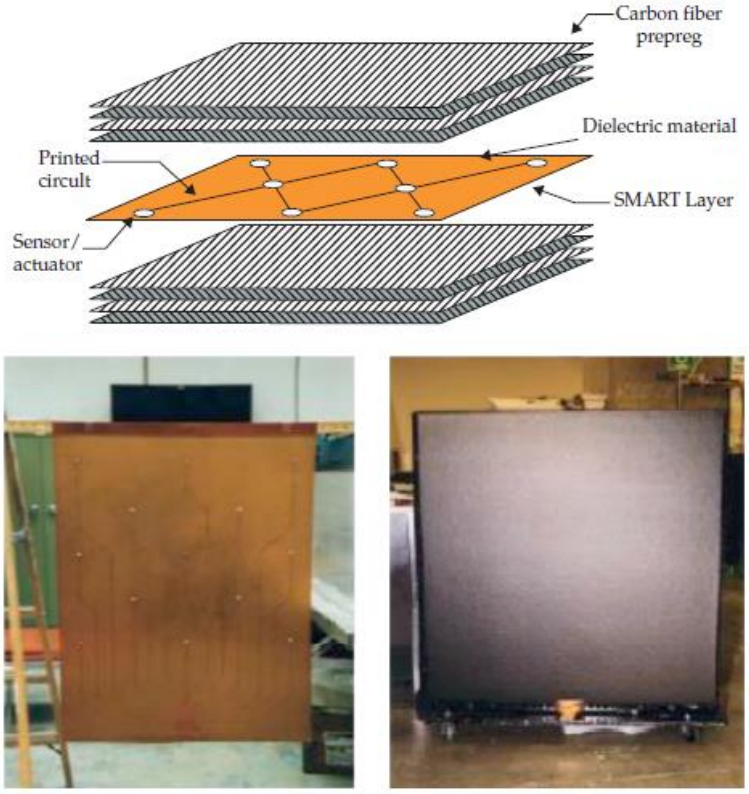

Figure 6: Piezoelectric Wafer Active Sensors

Impact detection is made with a piezo wafers network, as well as using the piezo wafers as both transmitters and receivers of guided Lamb waves for composite damage detection. In lamb wave method elastic waves propagate the shape and frequency of reflection in solid structures depending on material, thickness and boundary conditions. SHM methods use lamb waves to represent specific properties such as voids, fatigue cracks and sample debonding which needs high initiative to efficiently and accurately reconstruct the detected signals. Lamb wave method is good at surface penetration but this systems process for to get meaningful result is complex [9].

2.2.4 Electrical Property Sensors

SHM methods that use electrical properties of composite structures depend on the material itself to behave like sensor. Epoxy resin is an insulator and carbon fibers are electrically conductive materials. The carbon fiber reinforced polymer (CFRP) composite is conductive due to densely packed carbon fibers contact each other. In case of structural damages such as crack and delamination, the electrical conductivity

is expected to change. Glass fiber reinforced polymer (GFRP) composites are insulator materials that have special dielectric properties. Since the dielectric permittivity of air will be different from GFRP, the delamination and cracks occurring in the structure cause the dielectric properties to change.
For electrical SHM two different way was determined:

1. Electrical Resistance and Electrical Potential Methods for Composites SHM
2. Frequency Domain Methods for Electrical SHM of Aerospace Composites

2.2 An Analysis of Structural Health Monitoring with Novel Approaches Using CNT's

In addition to traditional SHM methods, utilization of nanomaterials like CNTs and graphene for SHM bring a different approach. In consequence of their multifunctional properties and their small sizes with low density, CNTs are attractive materials. In the aerospace industry, where lightness is an important parameter, CNT has no competitor due to its good mechanical and electrical properties as well as being a light material.

CNTs are electrically conductive up to hundreds of Siemens per meter and also particularly stiff and strong, up to 1 TPa and 63 GPa respectively [10]. To compare, CNTs are 100 times stronger than steel and can have metallic conduction 100 times more than copper over micron distances [11].
The improved conductivity and mechanical properties of CNTs have enabled them to be used in SHM methods to simultaneously monitoring strain situation. Electrical resistance of CNTs increases when damage occur.
It has been observed that the change in the resistance of CNTs with the effect of strain varies between 5% and 100% depending on how CNTs are regulated, produced, which matrix system is used and how the samples are mechanically deformed [12]. CNTs can be integrated with several methods, or applied to the surface of the composite. Instead of integrating the CNTs into the inner structure of the composite, the CNT we apply as a sensor to its surface is a simpler and more attractive method. Various studies such as surface painting with special paint or Bucky-paper paste onto surface have been carried out on this subject.

2.3 CNT Materials

CNTs are cylindrical graphene sheets which contain bonded carbon atoms. Each CNTs consist of one or more layers of graphene and is named according to the number of layers it contains such as single wall, double wall or multiwall CNTs.

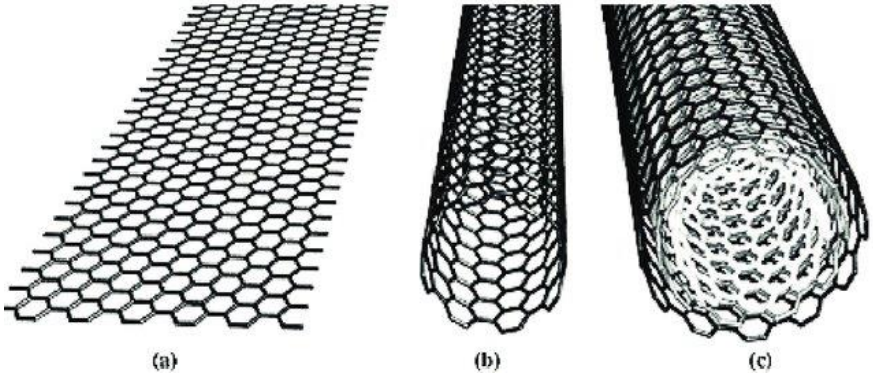

Figure 7 : a)Singlewall CNT b)Doublewall CNT c)Multiwall CNT

With high electrical, mechanical and thermal properties, carbon nanotubes (CNT) have a lot of potential usage from giant mechanical structures to electrical devices. These wide enforcement field of CNTs attract the industries and researchers, this situation increase the number of publications and patents. This enhancement lead to an expansion on application areas of CNTs. Increase of fabrication capacity and number of patents and publications year-by-year basis shown in figure.

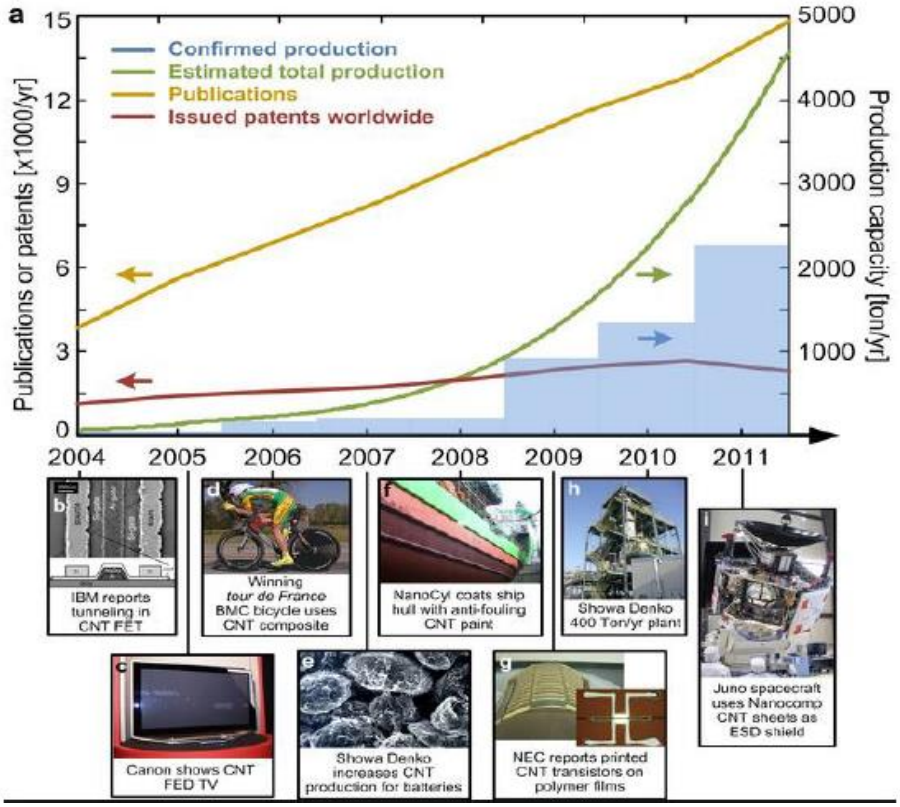

Figure 8: CNT Fabrication Capacity and nNumber of Patents and Publications

The high aspect ratio of CNT provides wider opportunities for processing shear force materials to give anisotropic properties; A critical advantage that can benefit from dispersion to colloidal nanomaterials.

2.4.CNC Materials

Cellulose nanomaterials are considered strong materials. The elastic modulus of individual cellulose nanofibrils varies between 65 GPa and 145 GPa depending on the raw material and measurement method. The elastic modulus of cellulose nanocrystals is around 137-150 GPa 3, besides, the value of bacterial cellulose fibrils varies between 78-114 GPa. If we compare these values with those of aluminum, the elastic modulus of aluminum is 69 GPa, 200 Gpa of steel and 69 GPa of glass. Due to its hydroxyl (OH) surface, cellulose is a hydrophilic material. Water adsorption and retention of cellulose nanomaterials are enhanced by high specific surface areas. Depending on the application, water absorbency can be a positive or negative feature.

In general, NFC-based materials have superior mechanical properties than NCC because of the higher aspect ratio of NFC. In addition, the efficiency of NFCs (~ 100%) is superior to NCCs (~ 50%). CNCs typically have a few nanometer diameters and their length varies from 10 to 500 nm, while CNFs have a diameter of 3–50 nm and several micrometers in length.

Cellulose nanofibrils can be used in substrates for printed electronics, with or without fillers. Filling pastes consisting of wood fibers, cellulose nanofibrils and filler materials (up to 40%), as well as pigment composites containing 80% filler and 20% CNF have proven to be good surfaces for printed electronics.

3. EXPERIMENTAL METHOD

3.1. Fabrication of CNT/CNC Solutions

CNT/CNC solutions with different weight ratio was fabricated. On the other hand, the most suitable concentration on the composite plate was chosen as 1.0 wt%CNT 1.0 wt % CNC.

In first step, pure multiwalled carbon nanotubes (MWCNT) with small diameter (5-15 nm) dried in the oven at 80 ºC for 48 hours.

Figure 9:Multi-Walled Carbon Nanotube

Assay	≥98% carbon basis
Form	powder
O.D. × I.D. × L	10 nm ± 1 nm × 4.5 nm ± 0.5 nm × 3-~6 µm, TEM
Surface area	280-350 m^2/g (BET)
Mp	3652-3697 °C (lit.)
Density	~2.1 g/mL at 25 °C (lit.)
Bulk Density	0.068 g/cm^3

Table 1: MWCNT Properties

The product of CelluForce company Cellulose Nanocrytals (CNC) was used. This product's chemical name is cellulose sulfate sodium salt.

Figure 10:Cellulose Nanocrytals (CNC)

50 mL of CNT / CNC solution containing 1.0 wt% CNT, 1.0 wt% CNC was prepared by adding 0.5 g CNT and 0.5 g CNC to water. Tapered microtip with 3mm tip diameter ultrasonic homogenizer (SONICS) was used for homogenization. A 50 mL CNT/CNC solutions were mixed for 1 hour at 30% amplitude having a 20 secs on and 30 secs off pulses. The solution cup was placed in an ice bath to keep the solution temperature constant.

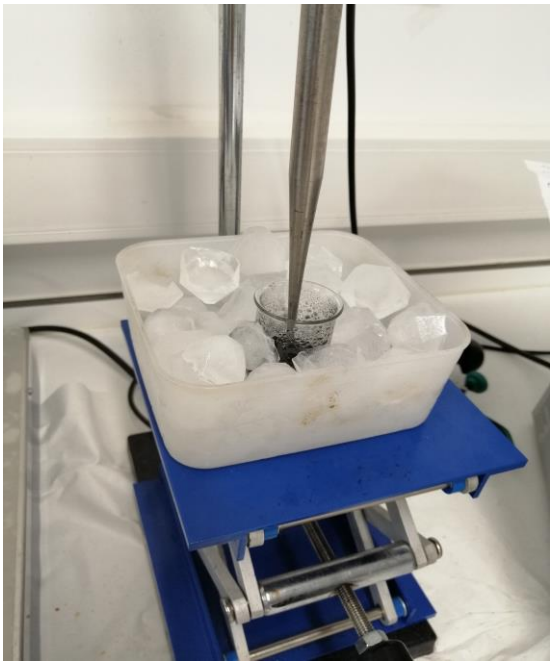

Figure 11:Homogenization of Solution with Sonicator

3.2. Characterization of CNT/CNC Solutions

3.2.1. Rheological Properties Measurement

With the rheology test, the internal response of the materials to the forces is analyzed, and the deformation of the substance is measured under the influence of the exposed pressure. Solution flow properties are important in all transformation and production processes: material is forced to flow and rheological properties determine machinability.

First, flow is included in the fabrication and processing of such materials to form useful materials. Therefore, fluid rheology determines pressure levels in processes such as extrusion, calendering, fiber spinning and layer aeration. Similarly, rheology residual pressures affect cycle times and gap formation in composite machining processes such as pneumatic molding, pressure molding and injection molding. Secondly, mechanical properties are very important in the use of the solution and mechanical behavior is also affected by rheology. In addition, rheological measurements are used to determine the properties of the product and quality control processes. Such measurements are used to evaluate and understand the interaction of different components of a multi-component and multi-phase mixture and their effects on flow and other properties of such materials [15].

3.2.2. Electrical Resistivity Measurement

While the electrical resistance is generally measured with a multimeter, the relative electrical resistance variation $\Delta R / R$ can be measured through with an electrical bridge (Figure) similar to that used to read the electrical resistance strain gauges. DC or AC excitation can be utilizied. First, it avoids the possible effects of parasitic capacitances and inductances; the latter avoids the polarization-induced error and can mitigate the effects of nonlinear resistance, so it is sometimes preferred in mesaurements.

Four-point detection method (4-terminal, 4-wire, 4-probe, etc.) can be used to increase accuracy (Figure 7b); this method may be more accurate because it uses a separate current carrying path (1-4) and voltage sensing path (2-3) so that the additive wiring and contact resistors can be eliminated [16].

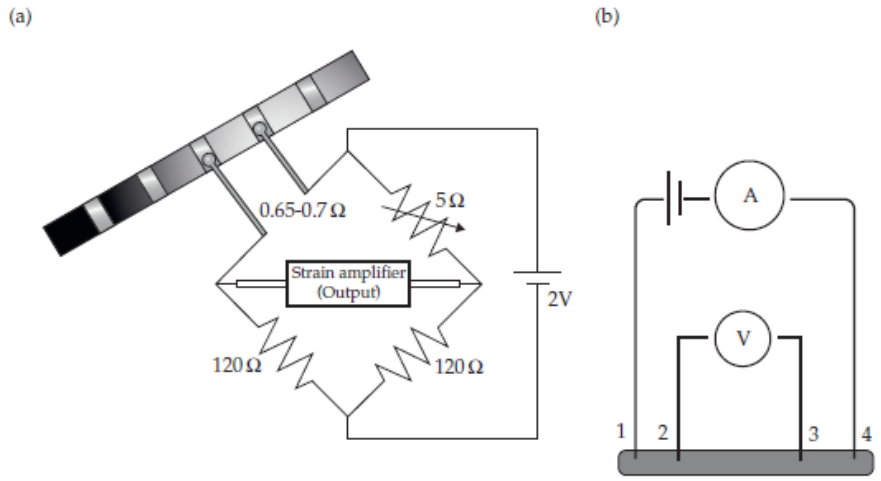

Figure 12: (a) strain gage bridge circuit (b) four-point probe

First electrical resistance measurement method; strain gage bridge circuit for measuring directly the relative change of electrical resistance; the second one is four-point measurement of resistance between voltage sense connections 2 and 3 current is supplied via connections 1 and 4.

The electrical resistance method includes the electrical resistance measurement between two points on the composite structures. To determine the damage location, several types of surface interpolation techniques are applied to the electrical resistance values measured at these locations. Conductivity mapping approach using a series of contacts across the surface of the CFRP composite [17].

Measurements can be made between each of its neighbors in the array by a contact to give conductivity values for each of these aspects. By drawing the conductivity values on the sample area and looking for abnormalities on the conductivity surface, we can identify possible damage areas.

For the calculation of the resistivity (ρ) and conductivity (σ) value independent of the geometry of the sample whose resistance value is determined in the Four-Probe device the equations shown in below are use:

$$\rho=F1*F2*F3*\pi\ln 2*t*R$$

$$\sigma=1/\rho$$

Here, t is the thickness of the sample, R is the resistance value determined by the device, and F_x is the geometric correction coefficient. This correction coefficient F1, which relates to the sample thickness, is taken into account at the comparable thickness values (t) between the 4-point probe tips.

In FPP 470 device, the length between the needle tips(s) is equal to 1mm. If the measured sample thickness is close to this value, the F1 coefficient should be calculated.

$$F_1 = \frac{\ln 2}{\ln\{[sinh\,(\frac{t}{s})]/[sinh\,(\frac{t}{2s})]\}}$$

The value of this coefficient can be calculated by the function. If t / s <1/5, it takes the value F1 = 1. Accordingly, it is not necessary to calculate this coefficient with very fine examples. In thicker samples, if t / s> 4, the coefficient to be calculated converges to F1 = 2 · ln2 · (s / t) [18].

F2 coefficient is related to infinity surfaces and F3 coefficients related to geometry of surfaces. For our study t/s ratio smaller than 1/5 so k considered equal to 1.

3.3. Fabrication of GFRP Composites

It was decided to produce with vacuum infusion method for the production of GFRP composite plates. Firstly, 4 plies glass fiber unidirection fabric were cut at required dimensions (300mm*300 mm). Then, these steps are followed;

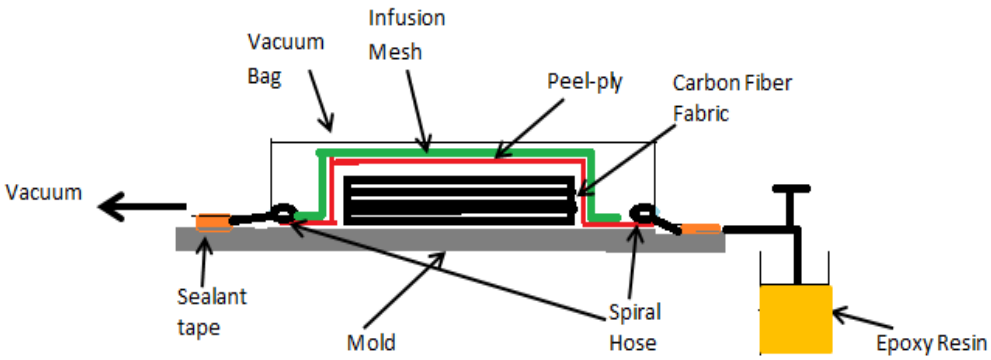

Figure 13:Vacuum Infusion Method

Vacuum Infusion Method:

1. Clean metal surfaces with acetone
2. Place the vacuum tape on the edges
3. Apply mold release agent
4. Place unidirectional glass fiber fabrics in 0^o-90^o-0^o-90^o degrees
5. Put PeePly onto glass fiber fabrics
6. Put mesh onto PeePly
7. Place spiral cables to opposite sides of the metal plate
8. Cover metal plate with vacuum bagging material
9. Vacuum the air inside the vacuum bag
10. Infuse epoxy resin into the system
11. Finish infusion when all fabrics are wetted

In order to curing, plate was waiting for 24 hours at room temperature 25^o.

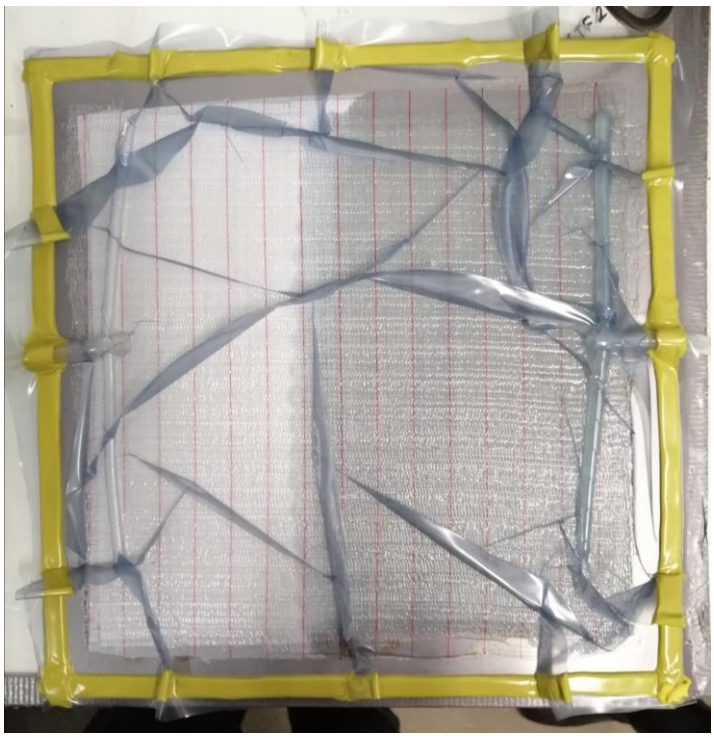

Figure 14:Fabrication of GFRP Composite Plate

According to American Society for Testing and Materials (ASTM) standarts, the dimensions of the specimens to be applied tensile test should be 25cm*2. 5cm.The cured 30*30cm GFRP composite plate was cutted appropriate dimensions by using CNC cutting machine.

Figure 15: Sizing of GFRP Composite with CNC Machine

3.4. CNT/CNC Screen Printing Procedure onto GFRP

Screen printing is a way of printing serially. This art branch, which dates back to very old times, has gained great importance in the branding of industrial products with the development of industry recently. The graphic, which has to be printed after covering different types of polyester silk fabric stretched to a wooden or metal frame with a film layer called photofilm emulsion and exposed in the light, appears as a template on this fabric. The photosensitive areas are emptied with the help of water and a sensitive template is formed. This template is called a pattern. Printing is done with the help of a squeegee (a rubber with a sharp mouth).

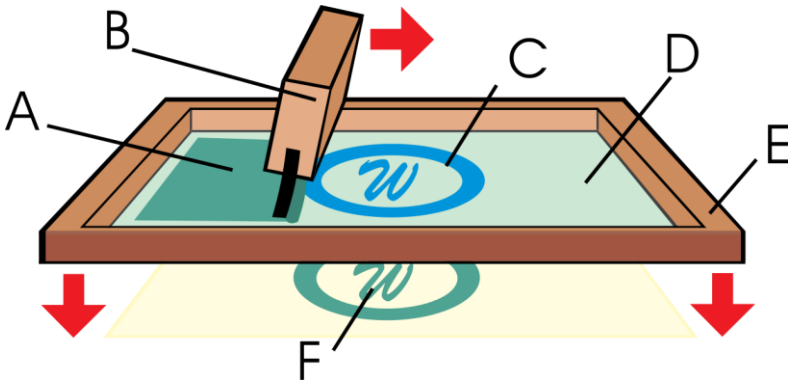

Figure 16: A. Ink B. Squeegee C. Image D. Photo-emulsion E. Screen F. Printed pattern.

Screen printing can be applied to all kinds of materials and surfaces. At the same time, printing on materials such as metal, ceramic, fabric and glass, which the printing press cannot print, is done by screen printing. It is the backbone of electronics. Thanks to screen printing, circuit boards are made clearer and cleaner. In recent years, it has become one of the indispensable parts of screen printing industry [19].

Polyester silk fabric mesh size changes according to the pattern desired to be printed on the surface. If pattern is complex mesh count must be more than basic pattern. However, meshes that have small size complicates the transition of solution to surface. For this reason, the mesh number is optimized and 55T polyester silk fabric was used.

For this study, the shape on the fabric is the sensor pattern that we will examine the change of resonant frequency. The screen printing frame is fixed on a flat surface with the locking bar clamp to keep the composite plate stable and prevent air bubbles during solution application.

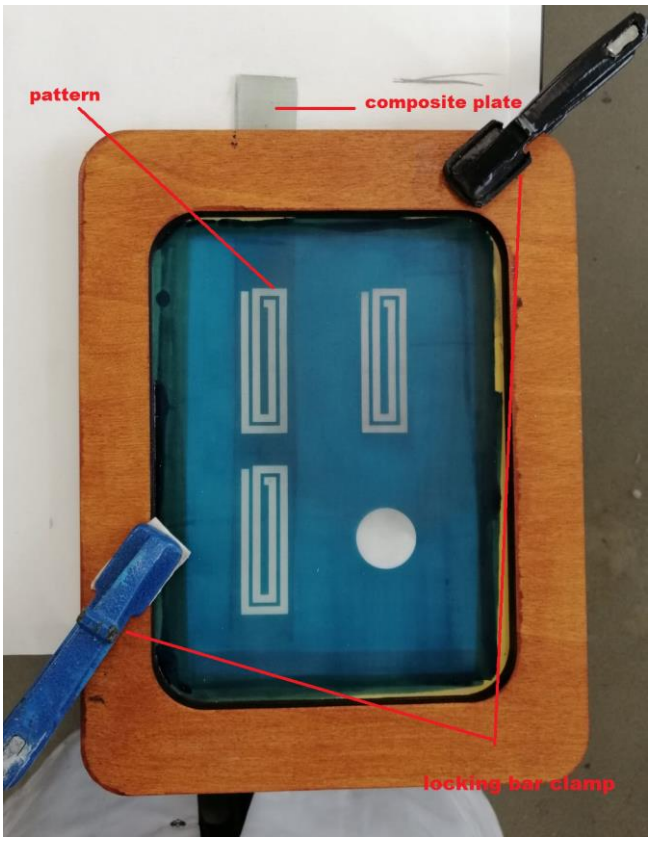

Figure 17:Screen Printing Equipment

Then 1.0 wt% CNT / CNC solution was applied on composite. During the application, air was applied with a dryer at a distance of 15 cm for 30 seconds to allow the paint to penetrate the surface better.

While applying the 1.0 wt % CNT/CNC solution on the composite surface, the problem of adhesion to the surface was encountered. As a solution to this problem, the surface was wetted with isopropylalcohol(IPA) prior to the application. IPA; It is a colorless, low boiling chemical and completely soluble in water. IPA is used as a solvent in vegetable oils and dyes, cellulose derivatives, fuel oil as an anti-freeze and extraction processes [20]. The figure below shows two prints made with IPA application and made without applying IPA.

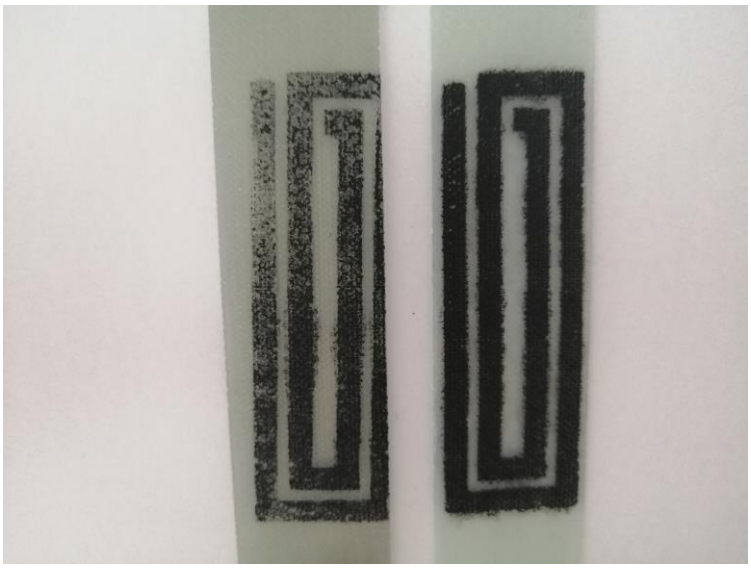

Figure 18:Effect of IPA Application

3.5. Mechanical and Electronic Tests

3.5.1. Tensile Test Mechanism

Tensile testing, one of the most common test methods, is used to determine the behavior of a sample when applying an axial tension load. Such experiments are used to determine the tensile properties of a material. This test is used for metals, plastics, elastomers, paper, composites, rubbers, fabrics, adhesives, films, etc. performed on a variety of materials, including.

It is widely used to determine the maximum load (tensile strength) a material or product can withstand. This test can actually be considered as a varying length with a loaded force. The sample that we want to be subjected to the tensile test is placed in the machine's grips and compressed. Thanks to this system, which is mostly integrated with computers, the amount of force and elongation appears with a graph.

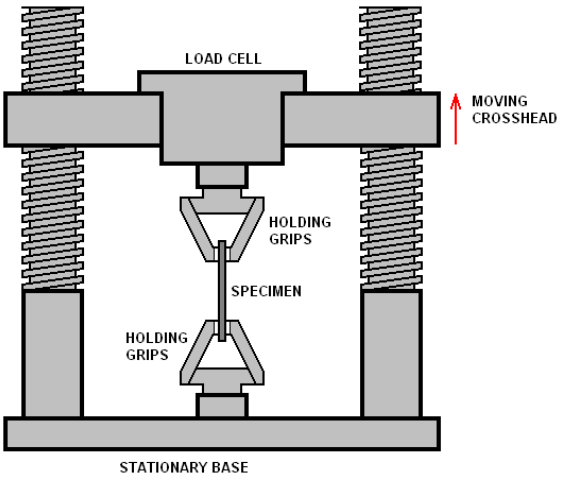

Figure 19:Tensile Test Procedure

All materials consist of an atomic community. Elasticity can be best understood by imaging that atoms are bound by arcs. When pulling the material, the arcs between atoms become longer and the material becomes longer. The elastic part of the curve is a straight line. A straight line indicates that the material will return to its original shape when the load is lifted. That is, if you remove the load applied to the material while it is in the elastic zone, the material returns to its original state.

The area after the elastic region is the plastic region. In this region, even if the load applied to the material is removed, the sample cannot be restored.

This study tensile test, done with specimens which prepared according to ASTM D3039 Test Method for Standard Tensile Properties of Polymer Matrix Composite Materials by UTM Tensile Test Machine.In this study, we stay in the elastic region for the composite plate.

Figure 20: Shimadzu AGS-X Universal Testing Machine (equipped with 50 kN load cell)

Loading speed was 1 mm/min. Loading was applied upto 3.437 kN two minute. The force graph applied depending on the time is shown in the figure below.

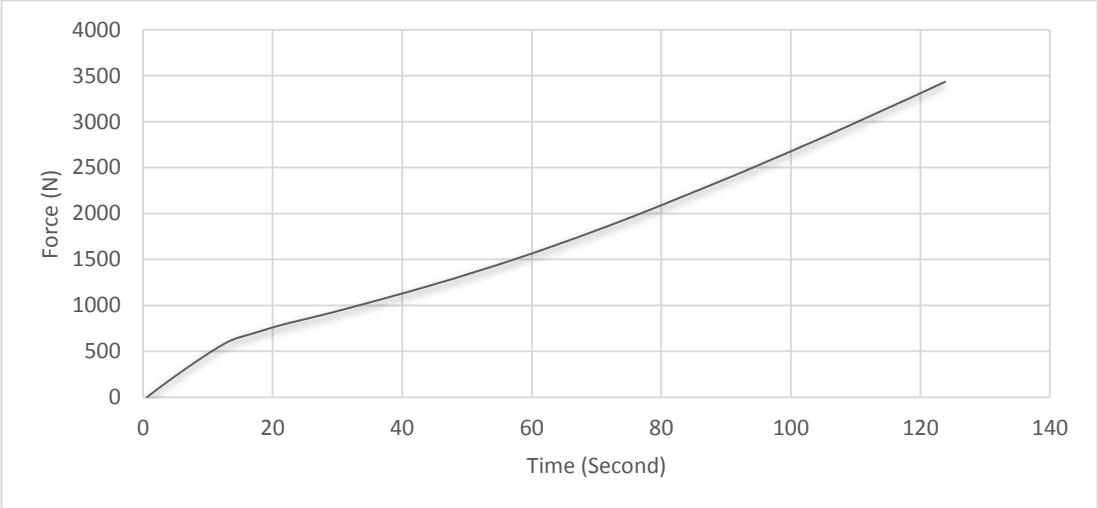

Figure 21: Force-Time Graphic of Tensile Test

According to the results of this test, the stress/strain curve of the composite plate was drawn as shown in below.

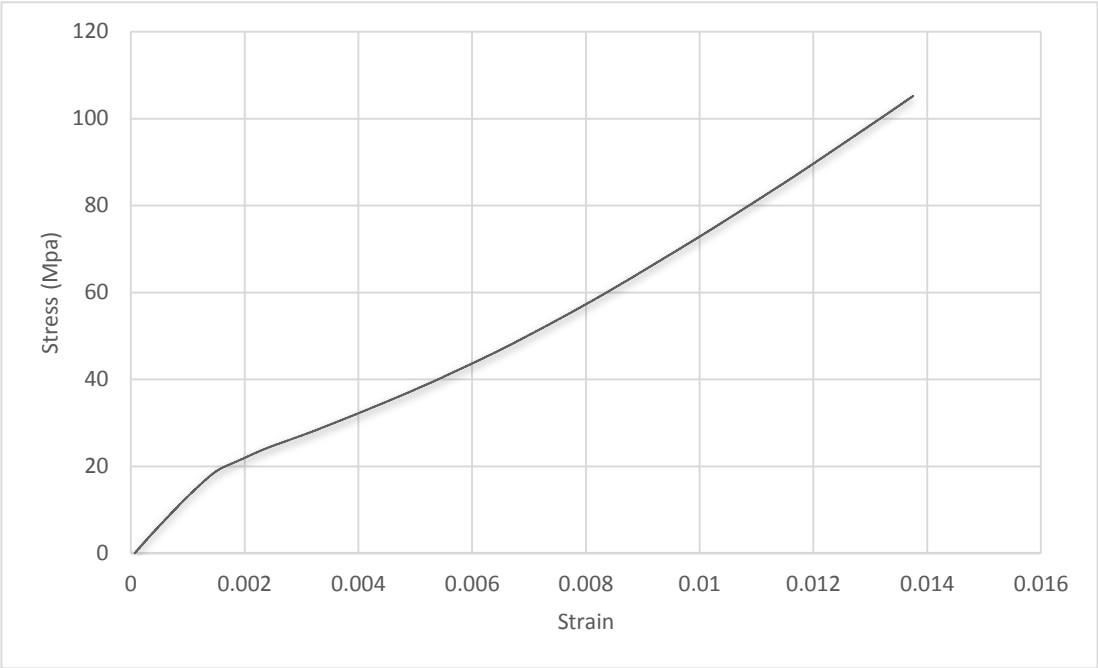

Figure 22:Stress-Strain Graphic of Tensile Test

As seen in the graphic, the stress applied on the sample increased up to 100Mpa. The maximum strain against this stress value is 0.014. Using the slope of the graph, the elastic modulus value of the GFRP composite plate can be found to be approximately 7.649GPa.

Main purpose in this study is to find the elongation caused by the tensile loads on the sample and to change from the shape change on the pattern caused by this elongation to frequency change. The dimension change of composite plate that occurs depending on the force is shown in the graphic below.

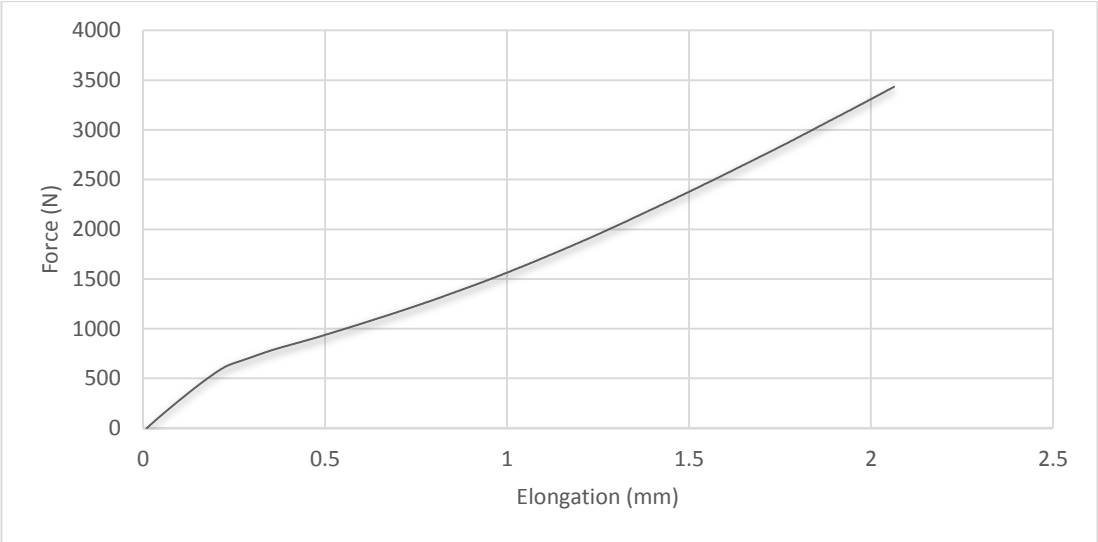

Figure 23:Force-Elongation Graphic of Tensile Test

The data obtained from the force-elongation plot will be used to detect the frequency change analyses.

3.5.2. Radio Frequency Identification Systems Simulation

In Radio Frequency Identification (RFID) technology, RFID tag and RFID reader are the most critical components. We can also add RFID printer, RFID antenna, software to be used by the system. An RFID tag consists of chip, power supply and antenna. This allows the tag to communicate with RFID readers and transfer and receive data. RFID is the name given to the technology that works with radio frequencies, which allows the tracking of the movements of an object carrying a label equipped with a microprocessor and the identity structure it carries on this label.

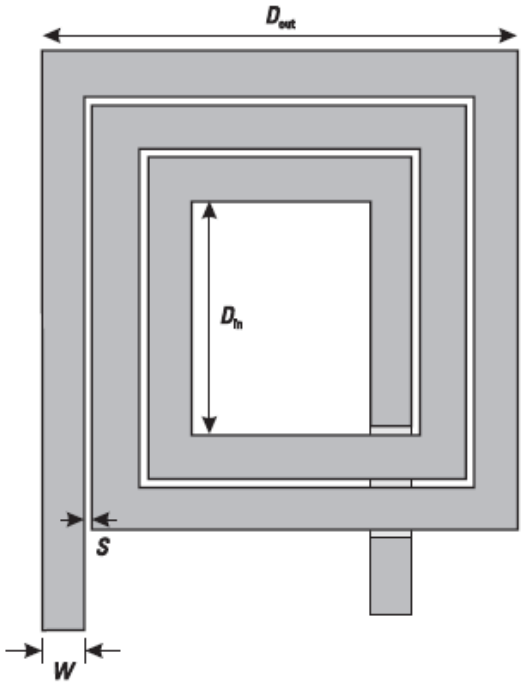

Figure 24:Antenna Pattern Model

In this study, we tried to produce an RFID radio microstrip antenna printed on a composite plate. There is a resonance frequency that varies according to the dimensional parameters of the produced RFID radio microstrip antenna. The values used by the AWR Simulation program used to determine the resonance frequency are described below.

$$f = \frac{1}{2\pi\sqrt{LC}}$$

As can be seen, the change of resonance frequency depends on the inductance (L) and capacitance (C) values in the denominator.

$$L = 2.34\mu_o \frac{n^2 d_{\text{avg}}}{1 + 2.75\psi}$$

$$d_{\text{avg}} = \frac{1}{2}(D_{\text{out}} + D_{\text{in}}) \quad \psi = \frac{(D_{\text{out}} - D_{\text{in}})}{(D_{\text{out}} + D_{\text{in}})}$$

The inductance value varies depending on the dimensions of the outer and inner edge lengths of the antenna.

$$C_{IW} = \frac{\epsilon_0 \epsilon_r A}{d}$$

$\epsilon_0 \epsilon_r$: dielectric coefficient of space*dielectric coefficient of plate

A=area of antenna

d=space width

The capacitance value changes depending on the dielectric coefficient of the material l placed on the antenna and the space between the lines in the antenna pattern.

In this study, the effects of the elongations on pattern dimension developed due to the tensile test on the resonance frequency of the system will be observed by using AWR simulation tool.

4.RESULTS and DISCUSSION

4.1. CNT/CNC Solution Results

4.1.1. Rheological Properties Measurement Results

TA Instruments Hr-2 Discovery Hybrid Rheometer was used to measure the viscosity values of the 0.5 wt % CNT/CNC and 1.0 wt % CNT/CNC solutions we prepared.

Figure 25: TA Instruments Hr-2 Discovery Hybrid Rheometer

1.0 wt% CNT / CNC solution was used in this study because 0.5 wt% CNT / CNC of the solutions could not hold onto the surface because of the excess fluid.

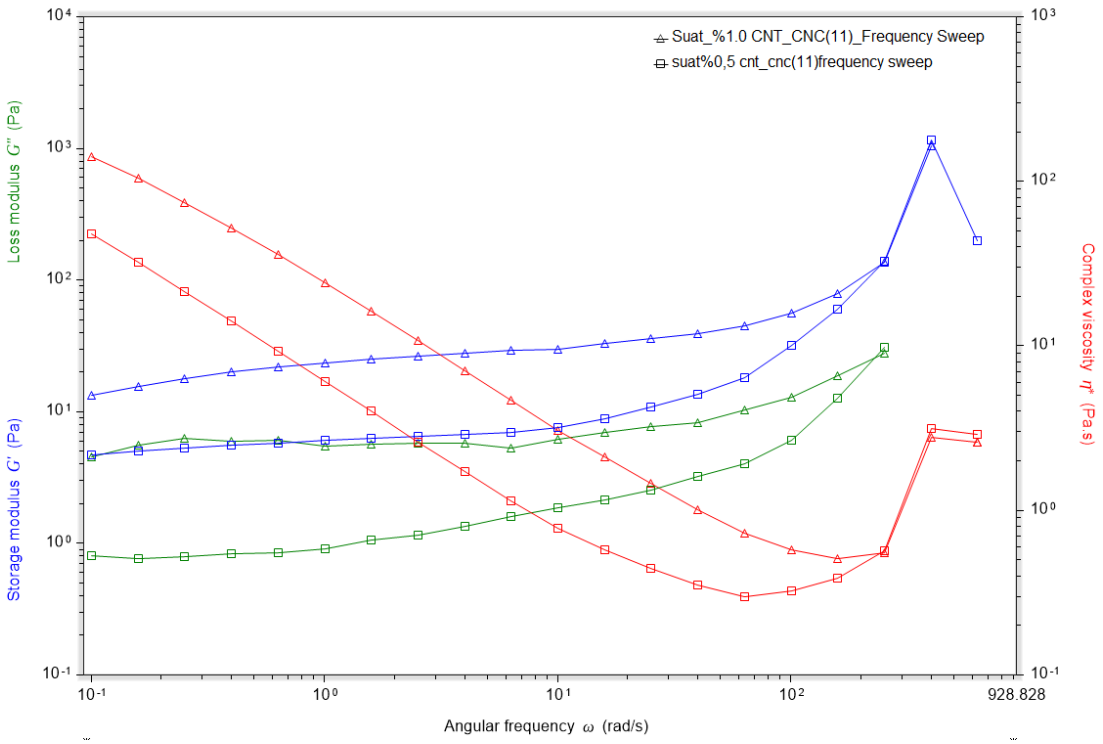

Figure 26:Rheology Results

According to the rheology results given, it was observed that the viscosity of 1.0 wt% CNT / CNC solution was approximately 10 times higher than 0.5 wt% CNT / CNC solution in the experiments performed at the same angular velocity.

4.1.2. Electrical Resistivity Measurement Results

The resistance measurements of the pattern printed on the composite with 1.0 wt% CNT / CNC solution were made with the Four-Probe measuring machine. An average value was obtained with the values from 5 different locations of the pattern.

The working mechanism of the Four Probe device has already been explained below. Some parts of the device are shown below.

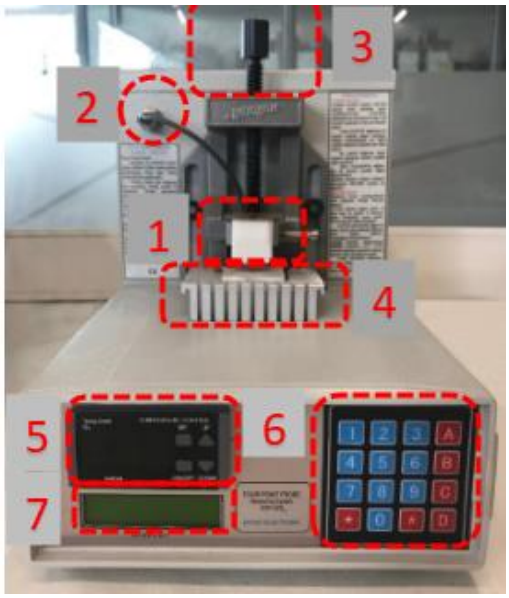

Figure 27:FourPoint Probe Testing Machine

1. Measuring tip (Needle or Fiber)
2. Probe cable connection
3. Measuring tip height adjustment
4. Measurement (and heating) tray
5. Heating control unit
6. Measurement control panel
7. Information screen

For the resistance measurement of our pattern, whose wall thickness is set as 2 mm, the probe pattern with a width of 2 mm is placed as shown in the figure.

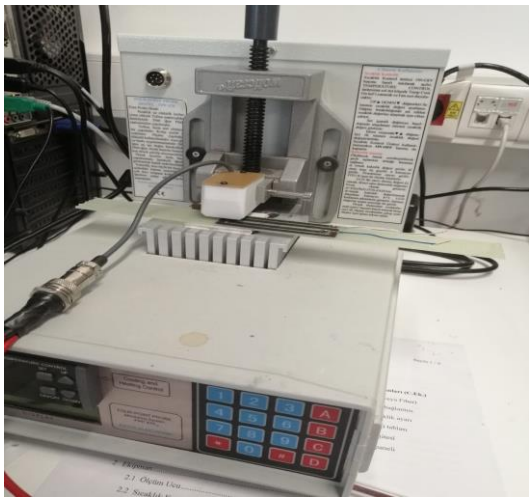

Figure 28:Resistivity Measurement of Solution

Conductive graphene ink (DZP Technologies) was applied, a commercial product, was used for reference at the beginning of the experiments. The resistance values of graphene ink printing on the composite are shown in below.

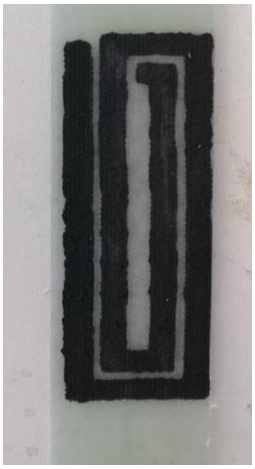

Figure 29:Pattern Printed with Graphene Ink

	1	2	3	4	5	Average
Resistivity (Ohm)	76.162	71.285	121.728	69.861	126.218	93.0508

Table 2:Resistivity Results Graphene Ink

Resistance values of 5 different samples that were printed with 1.0 wt% CNT / CNC solution was measured with four probe devices and their values are given below.

Figure 30: 1.0 wt%CNT/CNC Printed Patterns

	1	2	3	4	5	
Specimen 1 Resistivity (Ohm)	35.192	35.09	22.437	22.168	21.33	27.2434
Specimen 2 Resistivity (Ohm)	118.398	105.772	135.083	126.611	110.467	119.2662
Specimen 3 Resistivity (Ohm)	32.981	27.135	31.706	32.305	31.886	31.2026
Specimen 4 Resistivity (Ohm)	15.86	14.853	14.372	17.054	16.847	15.7972
Specimen 5 Resistivity (Ohm)	10.576	26.264	32.214	17.26	26.441	22.551
Average Resistivity						43.21208

Table 3: 1.0 wt%CNT/CNC Printed Patterns Resistivity Results

According to the values given in the table, the average resistance value of the produced 1.0 wt% CNT / CNC solution has been measured as 43.212 Ohms. It proves that we produce a solution with a lower resistance value and hence more conductivity than the commercial product graphene ink.

4.2. Change of System Frequency Under Tensile Loading

At the beginning of frequency analysis, our antenna pattern was designed in the electronic simulation program AWR. The pattern design with the edge lengths of 70 * 20 mm and the wall thickness of 2 mm between the lines is 1 mm, as shown below.

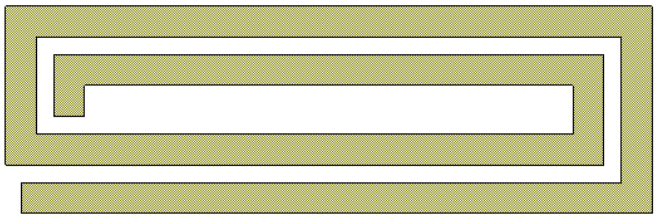

Figure 31:Antenna Pattern

The thickness of the GFRP composite sample required for the measurement is 1.36 mm, the pattern thickness is 0.02mm and the dielectric coefficient of the composite plate is 5.

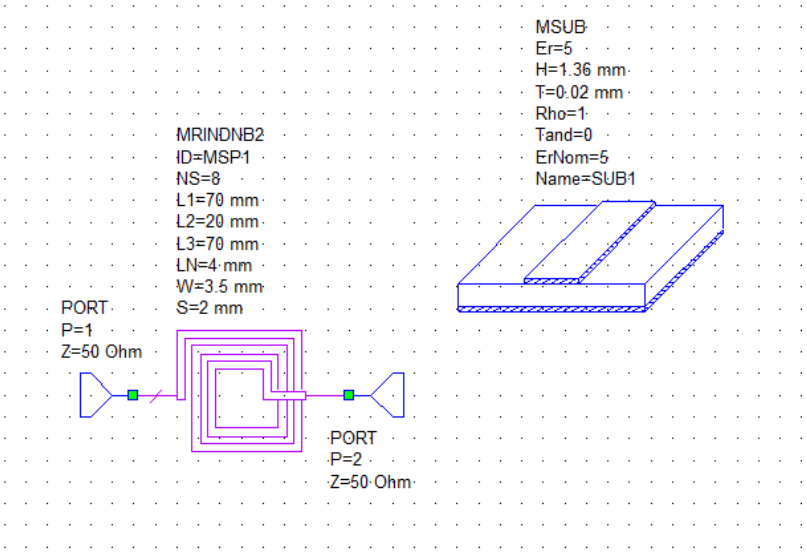

Figure 32:Antenna Pattern Design in AWR

The resonance frequency of the antenna pattern designed was calculated by simulating it in the AWR program and the result was found 591 MHz.

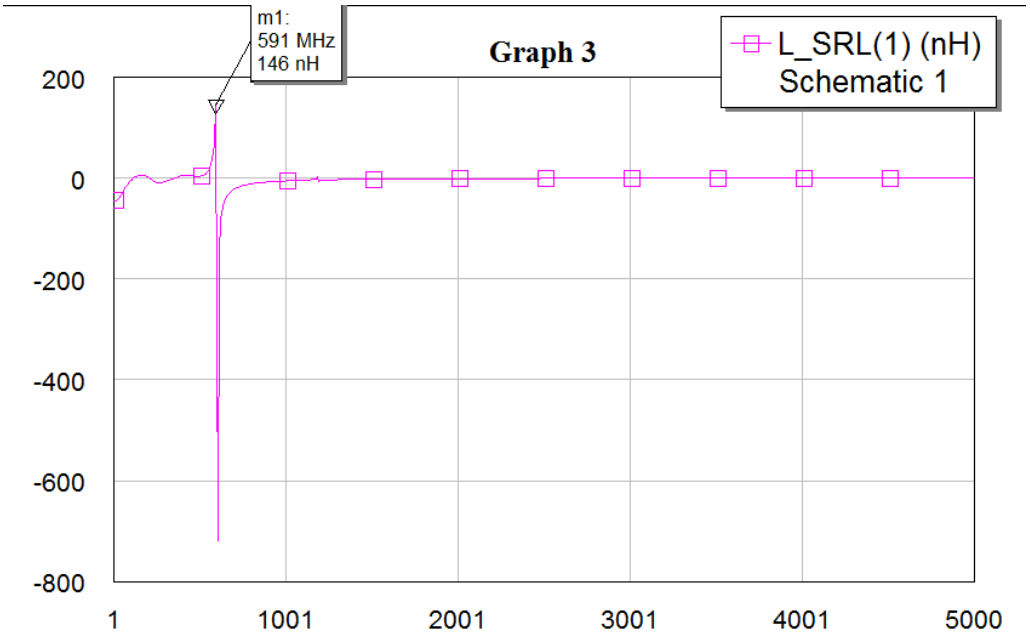

Figure 33:Resonance Frequency of Initial Pattern

Using the data obtained from the tensile test, elongation values were entered into the program and their changes on the resonance frequency were examined. When the obtained data is converted to a graph, there is a change in the resonance frequency when 1.3 mm elongation.

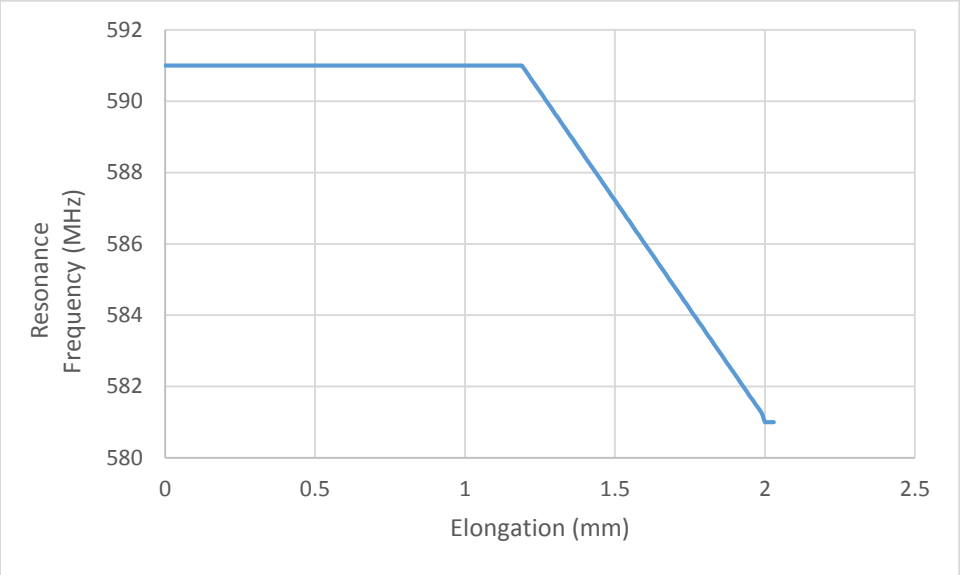

Figure 34:Resonance Frequency-Elongation Graphic

No changes were observed with respect to the degree of precision of the simulation in elongations of 0.5 mm and 1 mm, the changes in the resonance frequency in elongations of 1.5 and 2 mm are shown below.

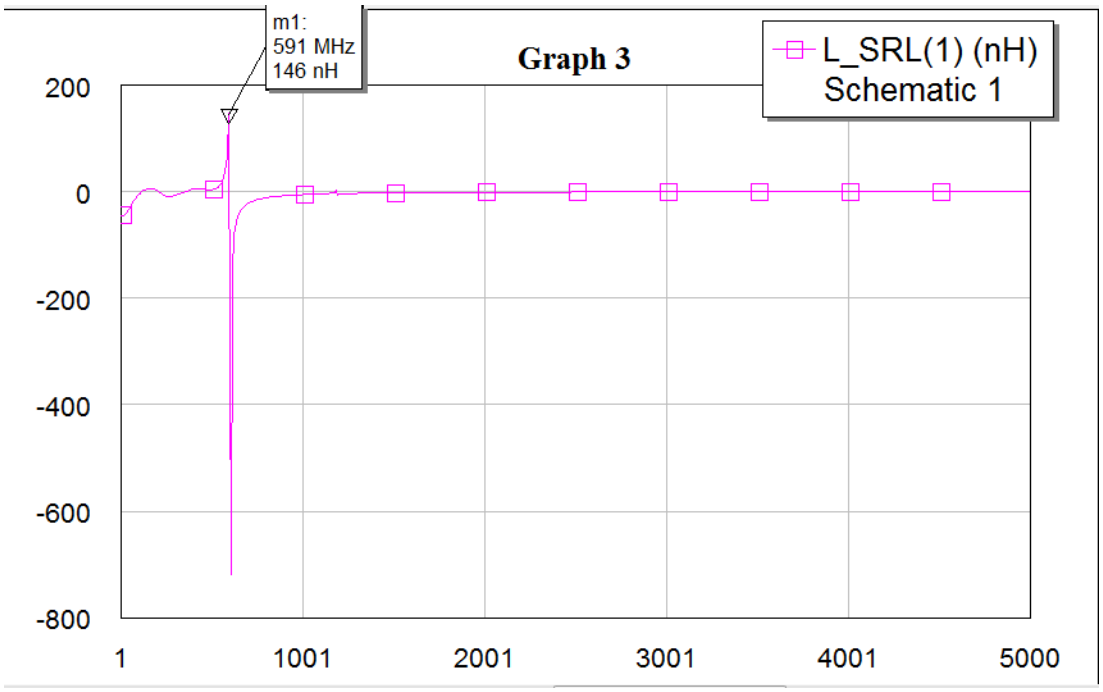

Figure 35:Resonance Frequency When 0.5 mm and 1mm Elongation Occur

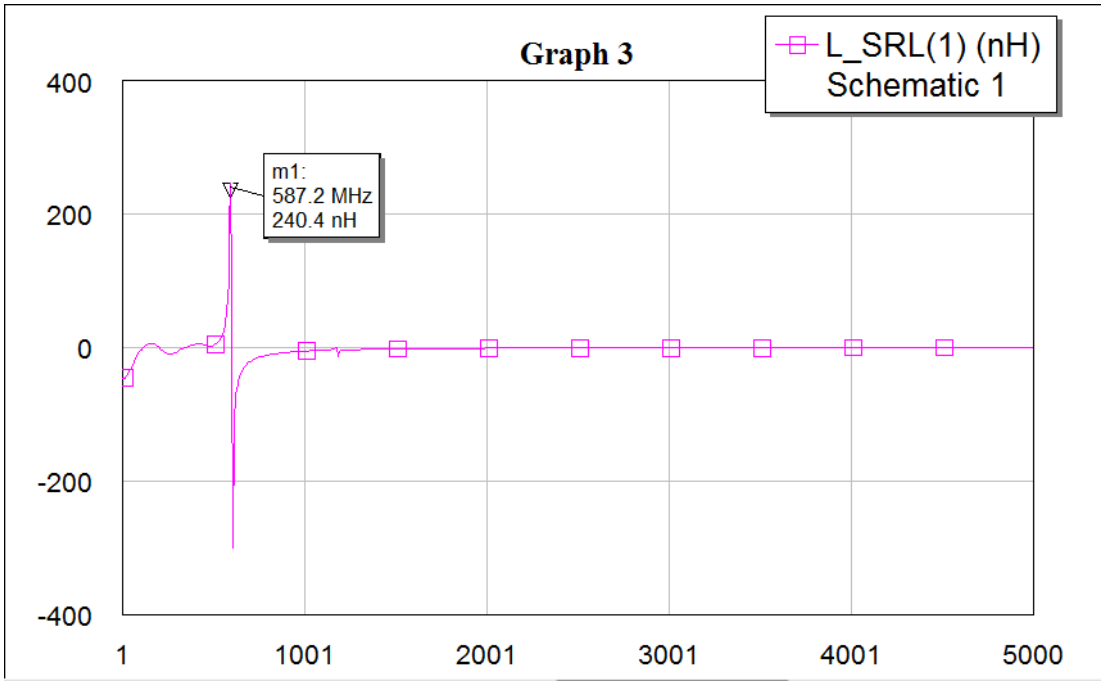

Figure 36: Resonance Frequency When 1.5mm Elongation Occur

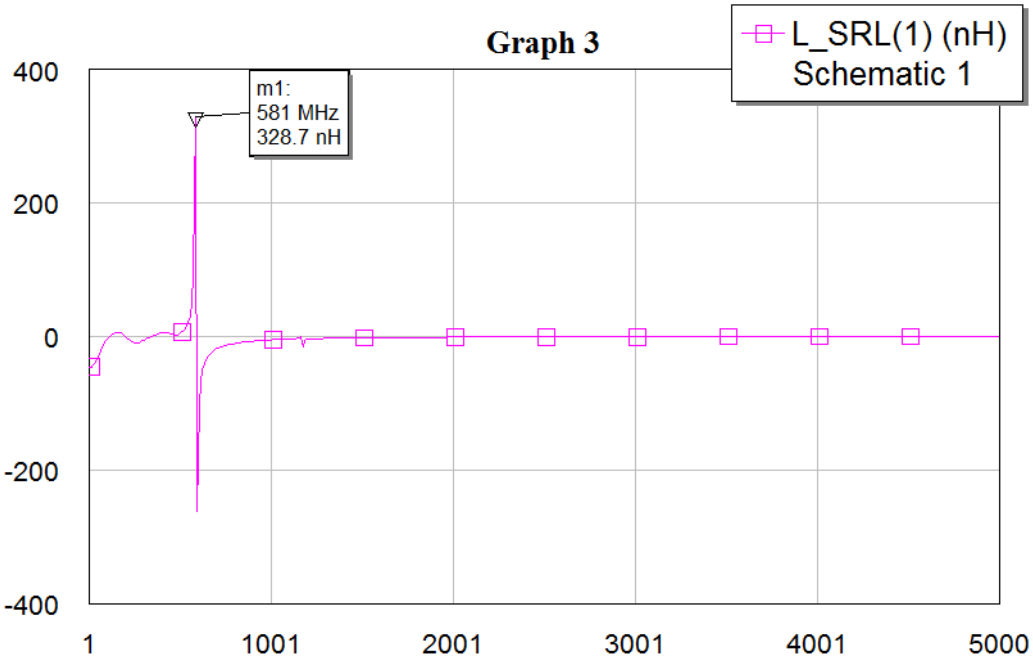

Figure 37: Resonance Frequency When 2 mm Elongation Occur

According to the results, the elongation in the length of the antenna pattern reduced the frequency at which it resonance after a certain threshold value.

5.CONCLUSION

In this study, a special paint was produced and the antenna pattern was printed on the composite plate by screen printing method. The effect of the resonance frequency of the antenna pattern on dimensional changes has been investigated. It has been observed that the resonance frequency decreases with elongations.

When there is any damage to the composite plates, the frequency change caused by the change in the length of the structure can offer us a new wireless undamaged inspection method.

In future studies,

1. Corona treatment can be applied for better adherence of the paint to the surface
2. Surface can be made smoother to reduce parasitic effects
3. Simulations can be developed to increase the frequency measurement range.

REFERENCES

1. Zhao, X., et al., *Ultrasonic Lamb wave tomography in structural health monitoring.* Smart Materials & Structures, 2011. **20**(10).
2. Coleman, J.N., et al., *Small but strong: A review of the mechanical properties of carbon nanotube-polymer composites.* Carbon, 2006. **44**(9): p. 1624-1652.
3. Nessim, G.D., *Properties, synthesis, and growth mechanisms of carbon nanotubes with special focus on thermal chemical vapor deposition.* Nanoscale, 2010. **2**(8): p. 1306-1323.
4. Chung, D.D.L., *Carbon materials for structural self-sensing, electromagnetic shielding and thermal interfacing.* Carbon, 2012. **50**(9): p. 3342-3353.
5. Iijima, S., *HELICAL MICROTUBULES OF GRAPHITIC CARBON.* Nature, 1991. **354**(6348): p. 56-58.
6. Endo, M., *The Growth Mechanism of Vapor-Grown Carbon Fibers*. 1975, University of Orleans: Orleans, France.
7. De Volder, M.F.L., et al., *Carbon Nanotubes: Present and Future Commercial Applications.* Science, 2013. **339**(6119): p. 535-539.
8. Inam, F., et al., *Multiscale Hybrid Micro-Nanocomposites Based on Carbon Nanotubes and Carbon Fibers.* Journal of Nanomaterials, 2010.
9. Yamamoto, N., R.G. de Villoria, and B.L. Wardle, *Electrical and thermal property enhancement of fiber-reinforced polymer laminate composites through controlled implementation of multi-walled carbon nanotubes.* Composites Science and Technology, 2012. **72**(16): p. 2009-2015.
10. Khan, S.U. and J.-K. Kim, *Improved interlaminar shear properties of multiscale carbon fiber composites with bucky paper interleaves made from carbon nanofibers.* Carbon, 2012. **50**(14): p. 5265-5277.
    Garcia, E.J., B.L. Wardle, and A.J. Hart, *Joining prepreg composite interfaces with aligned carbon nanotubes.* Composites Part a-Applied Science and Manufacturing, 2008. **39**(6): p. 1065-1070.
11. Qian, D., et al., *Load transfer and deformation mechanisms in carbon nanotube-polystyrene composites.* Applied Physics Letters, 2000. **76**(20): p. 2868-2870.
12. Thostenson, E.T. and T.W. Chou, *Aligned multi-walled carbon nanotube-reinforced composites: processing and mechanical characterization.* Journal of Physics D-Applied Physics, 2002. **35**(16): p. L77-L80.
13. Paul, D.R. and L.M. Robeson, *Polymer nanotechnology: Nanocomposites.* Polymer, 2008. **49**(15): p. 3187-3204.
14. Wicks, S.S., et al., *Multi-scale interlaminar fracture mechanisms in woven composite laminates reinforced with aligned carbon nanotubes.* Composites Science and Technology, 2014. **100**: p. 128-135.
15. 41. White, K.L. and H.-J. Sue, *Delamination toughness of fiber-reinforced composites containing a carbon nanotube/polyamide-12 epoxy thin film interlayer.* Polymer, 2012. **53**(1): p. 37-42.
16. 42. Wicks, S.S., R.G. de Villoria, and B.L. Wardle, *Interlaminar and intralaminar reinforcement of composite laminates with aligned carbon nanotubes.* Composites Science and Technology, 2010. **70**(1): p. 20-28.
17. Abry, J.C., et al., *In-situ monitoring of damage in CFRP laminates by means of AC and DC measurements.* Composites Science and Technology, 2001. **61**(6): p. 855-864.
18. 44. Lau, K.T., *Structural health monitoring for smart composites using embedded FBG sensor technology.* Materials Science and Technology, 2014. **30**(13A): p. 1642-1654.

19. 45. Torres Gorriz, B., et al., *Experimental and numerical analysis of a hybrid FBG long gauge sensor for structural health monitoring.* Measurement Science & Technology, 2014. **25**(12).